# Variations in Oligosaccharide−Protein Interactions in Immunoglobulin G Determine the Site-Specific Glycosylation Profiles and Modulate the Dynamic Motion of the Fc Oligosaccharides

Mark R. Wormald,* Pauline M. Rudd, David J. Harvey, Su-Chen Chang,‡ Ian G. Scragg,§ and Raymond A. Dwek

*Oxford Glycobiology Institute, Department of Biochemistry, University of Oxford, South Parks Road, Oxford OX1 3QU, U.K.*

*Received August 26, 1996; Revised Manuscript Received December 4, 1996*[⊗]

ABSTRACT: Glycoproteins, such as immunoglobulin G (IgG), consist of an ensemble of glycosylated variants, or glycoforms, which have different oligosaccharides attached to a common peptide. Alterations in the normal glycoform populations of IgG are associated with certain disease states, notably rheumatoid arthritis and its remission during pregnancy. In this paper, we show that two sets of IgG Fc glycoforms have quite different physical properties. The first set has 1,6 arm terminal galactose residues which interact with the protein, resulting in glycan binding to the protein surface, in agreement with the crystal structure. In contrast, the second set of glycoforms which lack galactose does not bind to the protein surface. Recently developed HPLC techniques combined with enzymatic digestion and mass spectrometry have been used to assign the glycan structures on IgG, Fab, and Fc. Comparison of Fab with Fc shows that glycosylation is site-specific. Two major glycan structures are present on Fab (fucosylated digalacto-bianntenary with and without bisect) and three on Fc (fucosylated agalacto-, 1,6 arm monogalacto-, and digalacto-bianntenary). In comparison to Fab, Fc glycans contain (i) lower levels of bisecting GlcNAc, (ii) lower levels of galactose, (iii) higher than expected levels of 1,6 arm galactose relative to 1,3 arm, and (iv) no 1,6 arm sialylation. We interpret these differences to indicate a role for both the protein quaternary structure and specific protein−glycan interactions in determining the glycoform populations. NMR relaxation measurements have been used to probe the mobility of the glycans in the Fc. By comparing two samples with different glycoform populations, we conclude that this mobility is dependent on the primary sequence of the glycan. Glycans carrying a galactose residue on the 1,6 arm have relaxation properties very similar to those of the peptide backbone and thus do not have independent motion. Glycans lacking galactose have relaxation rates 30 times slower than that of the peptide and thus a higher degree of mobility. These agalactosyl glycans do not interact with the protein, resulting in exposure of previously covered regions of the peptide surface and making the glycan more accessible. This implies that at the early stages of glycan processing the Fc glycans are mobile and only partially protected by the protein quaternary structure. Immobilization of the glycans occurs as a consequence of addition of galactose to the 1,6 arm and results in increased protection.

Immunoglobulin G (IgG)[1] is a glycoprotein (Dwek et al., 1995) associated with three types of complex biantennary glycans containing zero, one, or two galactose residues on their outer arms, commonly known as G0, G1, and G2, respectively (Figure 1). Within each class of IgG glycans, there are four species which result from the presence or absence of core fucose and "bisecting" GlcNAc. Further heterogeneity arises as a result of sialylation of some terminal galactose residues. IgG contains on average 2.4 glycans

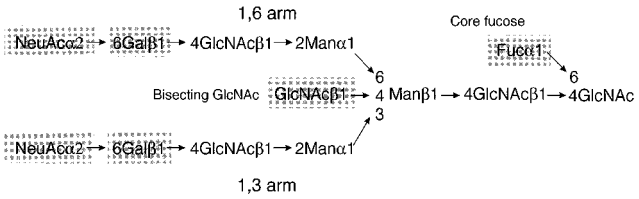


FIGURE 1: Schematic representation of the oligosaccharides found on IgG. The boxed residues can be present or absent. The following notation is used in this paper: G0, no NeuAcs or Gals are present; G1, one Gal and no NeuAcs are present; G1(1,*x*), the Gal present is on the 1,*x* arm; G2, both Gals and no NeuAcs are present; G2S, both Gals and one NeuAc are present; G2S(1,*x*), the NeuAc present is on the 1,*x* arm; G2S2, both Gals and both NeuAcs are present; F, core fucose is present; B, bisecting GlcNAc is present.

(Youings et al., 1996), of which 2 are conserved at Asn 297 in the $C_H2$ domain of the Fc region. The additional oligosaccharides are located in the hypervariable regions in the Fab.

The glycosylation of IgG Fc is known to be important both in its normal physiological role and in certain disease pathologies. Alterations in the incidence of nonreducing

* Corresponding author.

‡ Present address: Glyco-immunochemistry Research Laboratory, Institute of Molecular and Cellular Biology, Chang-Gung Medical College, 259 Wn-Hwa 1st Road, Kwei-san, Tao-yuan, Taiwan 33332.

§ Present address: Department of Paediatrics, John Radcliffe Hospital, Oxford OX3 9DU, U.K.

⊗ Abstract published in *Advance ACS Abstracts,* January 15, 1997.

[1] Abbreviations: 1D, one-dimensional; CD, circular dichroism; CID, collision-induced decomposition; CPMG, Carr−Purcell−Meiboom−Gill; ESR, electron spin resonance; gu, glucose units; HPLC, high-pressure liquid chromatography; IgG, immunoglobulin G; MALDI, matrix-assisted laser desorption/ionization; NMR, nuclear magnetic resonance; RA, rheumatoid arthritis; TOF, time of flight; G0(%), G1-(%), and G2(%), the percentage of complex biantennary oligosaccharides containing zero, one, or two galactose residues per molecule, respectively. For individual glycan nomenclature, see Figure 1.

S0006-2960(96)02147-2 CCC: $14.00 

terminal galactose residues have been associated with the occurrence (Parekh et al., 1985), early diagnosis (Young et al., 1991), and remission during pregnancy (Rook et al., 1991) of rheumatoid arthritis (RA). More recently (Malhotra et al., 1995), we have shown that aggregated agalactosyl IgG is capable *in vitro* of activating complement via oligosaccharide-mediated interaction with mannose-binding protein (MBP), providing a possible role for these oligosaccharides in the pathogenesis of RA. The presence of nonreducing terminal galactose residues is also important for binding of IgG to C1q and Fc receptors (Tsuchiya et al., 1989), and it has been shown that binding of monoclonal IgG rheumatoid factors to Fc is influenced by the Fc glycosylation but that binding does not directly involve the carbohydrates (Newkirk & Rauch, 1993).

X-ray crystallographic studies of the isolated Fc domain [human (Deisenhofer, 1981) and rabbit (Sutton & Phillips, 1983)] have shown that the two conserved oligosaccharide chains of the Fc are well defined, with the oligosaccharide 1,6 arms bound to the surfaces of the $C_H2$ domains (Figure 8, bottom left) and the rabbit structure showing additional extensive contacts between the two oligosaccharide 1,3 arms (not observed in the human structure). $^{13}C$ NMR (Rosen et al., 1979) and ESR spin labeling (Nezlin, 1990; Sykulev & Nezlin, 1990) studies have suggested that the Fc oligosaccharides have the same dynamic properties as the $C_H2$ domains. In contrast, X-ray crystallographic studies of mouse IgG Fab show only poorly defined electron density at the N-glycosylation site (Stanfield et al., 1990), indicating oligosaccharide mobility or disorder within the crystal. ESR spin labeling studies on IgM Fab (Lapuk et al., 1984) have shown the *N*-glycans to have a much higher degree of mobility than the peptide.

Structural investigation of the differences between IgG glycoforms has so far been limited to CD studies of normal and rheumatoid IgG. Differences between the CD spectra of intact normal and rheumatoid IgG have been interpreted in terms of a structural anomaly in the hinge region of rheumatoid IgG (Johnson et al., 1974), while CD studies on immune complexes from rheumatoid patients have suggested that only a portion of rheumatoid IgG contains these unusual structural determinants (Uesson & Hansson, 1982). Differences in papain cleavage rates have also been reported between rheumatoid and normal IgG (Watkins et al., 1970; Youings et al., 1996).

In this study, we have used recently developed normal phase HPLC techniques together with enzymatic digestion and mass spectrometry to characterize more fully the glycans on IgG, Fab, and Fc. This shows site-specific glycosylation of IgG with a relatively limited number of major glycans, two for Fab and three for Fc. Only one of these structures is common to both fragments. NMR relaxation measurements have been used to probe the Fc oligosaccharide−protein interactions, showing that the major interaction is between the 1,6 arm galactose residue and the protein surface. The differences in the site-specific glycosylation patterns between Fab and Fc can then be understood in terms of the protein quaternary structure and the nature of the oligosaccharide−protein interactions at each stage of the glycan biosynthetic pathway.

## MATERIALS AND METHODS

*Sample Preparation for Oligosaccharide Characterization.* Normal human serum IgG [prepared as in Parekh et al. (1985)] was cleaved by papain to Fab and Fc [as in Porter (1959) modified to give maximum cleavage]. Uncleaved IgG and Fc were separated from Fab by Protein G affinity chromatography (equilibration buffer, 0.1 M potassium phosphate at pH 7; elution buffer, 0.1 M glycine at pH 2.8). IgG and Fc were separated by gel permeation HPLC (Zorbax GF250; 0.1 M potassium phosphate at pH 7.2). Western blotting with αFab and αFc antibodies indicated that no Fab was present in the Fc preparation and vice versa. Normal serum IgG [G0(%) = 20] and purified Fab and Fc were desialylated and degalactosylated by incubating the proteins with *Arthrobacter ureafaciens* neuraminidase (2 units/mL) and *Streptococcus* 6646k (0.2 units/mL) in 0.05 M sodium acetate at pH 5.5 containing 10 mM $MnCl_2$ at 40 °C for 16 h (Kiyohara et al., 1976). The reactions were terminated by incubating the reaction mixture at 56 °C for 10 min. Oligosaccharides were released from normal and rheumatoid arthritis human serum IgG and its fragments by hydrazine using the Oxford GlycoSystems GlycoPrep 1000 apparatus. Released oligosaccharides were fluorescently labeled at the reducing terminal with 2-aminobenzamide (2AB) using a signal-labeling kit from Oxford GlycoSystems.

*HPLC Analysis.* GlycoSep-H and GlycoSep-N HPLC columns were obtained from Oxford GlycoSystems. Normal phase HPLC (Guile et al., 1996) was carried out using a GlycoSep-N column (size, 4.6 × 250 mm). Gradient conditions used were as follows. Solvent A was 50 mM ammonium formate at pH 4.4, and solvent B was acetonitrile. Initial conditions for gradient 1 were 20% A at a flow rate of 0.4 mL/min, followed by a linear gradient of 35 to 53% A over 132 min followed by 53 to 100% over the next 3 min. The flow rate was then increased to 1 mL/min over the next 2 min and the column washed in 100% A for 5 min, before being re-equilibrated in 35% A before injecting the next sample. The total run time was 180 min, and the column temperature was maintained at 30 °C. Elution positions in glucose units were calculated by comparison with a standard mixture of glucose oligomers. Integrals for partially resolved peaks were obtained by fitting to a Gaussian line shape.

*Matrix-Assisted Laser Desorption/Ionization Mass Spectrometry.* In-source decay (ISD) fragmentation MALDI mass spectra were acquired with a Micromass AutoSpec QFPD mass spectrometer (Micromass Ltd., Wythenshawe, Manchester, U.K.) fitted with an array detector and a nitrogen laser as described earlier (Bordoli et al., 1994). Oligosaccharide samples (1 μL) and the matrix solution [3 μL of a saturated solution of 2,5-dihydroxybenzoic acid (2,5-DHB) in acetonitrile] were placed on the mass spectrometer target and allowed to crystallize at room temperature. The crystals were then redissolved in ethanol and allowed to recrystallize (Harvey et al., 1994). Spectra were acquired with a laser pulse rate of 15 shots/s and a laser power of 160 μJ/pulse. The laser spot was scanned manually over the target surface in order to compensate for sample depletion. The array detector angle was set to the high-resolution position, and spectra were acquired with a resolution of about 2000 (FWHM). The mass range was *m/z* 500−2000 and resulted in 19 exposures of the array detector being needed to obtain

the full spectrum. Spectra were averaged until a satisfactory signal:noise ratio was obtained (usually 10−30 spectra).

Tandem mass spectral data were recorded with a Micromass AutoSpec mass spectrometer fitted with an orthogonal acceleration (OA) TOF mass analyzer (Bateman et al., 1995) with sample preparation as described above. The laser was operated at 10 Hz. Molecular ($MNa^+$) ions were selected with the magnetic sector and transmitted to the collision cell which used xenon as the collision gas and was operated to give a center-of-mass collision energy of 800 eV. The push-out pulse for the OA-TOF was synchronized with the laser pulse to give a delay equivalent to the flight time from the ion source. Fine tuning of the push-out pulse was achieved by observing the absence of the signal on a point detector situated after the OA-TOF when the push-out pulse was used. Ions were accumulated by the OA-TOF detector until a satisfactory signal:noise ratio was obtained. This process usually took about 20−30 min.

*Sample Preparation for NMR and Subsequent Analysis.* Human IgG was prepared from nonimmune serum from one normal control and one patient with rheumatoid arthritis, and the Fc fragments were obtained by papain digestion (Youings et al., 1996). The preparations were judged to be essentially homogeneous by polyacrylamide gel electrophoresis stained with Commassie blue and Western blotting using Fc-specific antibodies (data not shown). After the NMR studies, the oligosaccharides were released and purified as described previously (Ashford et al., 1987; Parekh et al., 1987). The incidences of agalactosylated [G0(%)], monogalactosylated [G1(%)], and digalactosylated [G2(%)] oligosaccharide structures were determined by Bio-Gel P4 chromatography using the standard method (Parekh et al., 1988).

*NMR Spectroscopy.* Samples for NMR were prepared by dissolving the protein (5 mg of normal, 10 mg of RA), lyophilized from $^2H_2O$, in 500 $\mu$L of $^2H_2O$. All spectra were recorded on a Varian Unity 500 spectrometer. Transverse relaxation rates ($T_2$) were measured using a CPMG (Meiboom & Gill, 1958) sequence (90°−{$\tau$−180°−2$\tau$−180°−$\tau$}$_n$−acq) with a 0.00025 s delay between pulses ($\tau$) and the total delay from first pulse to acquisition ($4\tau n$) varying from 0.001 to 0.256 s. Usually, 2000 scans were required for adequate signal:noise ratios. Spectra were Fourier-transformed directly with no prior mathematical manipulation.

*Analysis of $T_2$ Relaxation Data.* The total intensity ($I$) of three regions of the spectrum (aromatic, 6.19−7.80 ppm; aliphatic, 3.50−4.25 ppm; and methyl, −0.67 to 1.33 ppm) was measured as a function of total delay time ($t$). All resonances with a similar $T_2$ value within a given chemical shift region can be treated as a single $T_2$ component ($i$) with a transverse relaxation constant $T_{2_i}$ and an initial intensity ($I_i°$) equal to the sum of the individual resonance intensities. The intensity in any given region of a CPMG spectrum is then given by the summation over all the $T_2$ components within that region.

$$I(t) = \sum_i I_i° \exp\left(\frac{-t}{T_{2_i}}\right)$$

The experimental data [$I(t)$ versus $t$] were fitted to the above expression using a least-squares algorithm (Numerical Algorithms Group Ltd., routine E04FDF) and minimizing the function

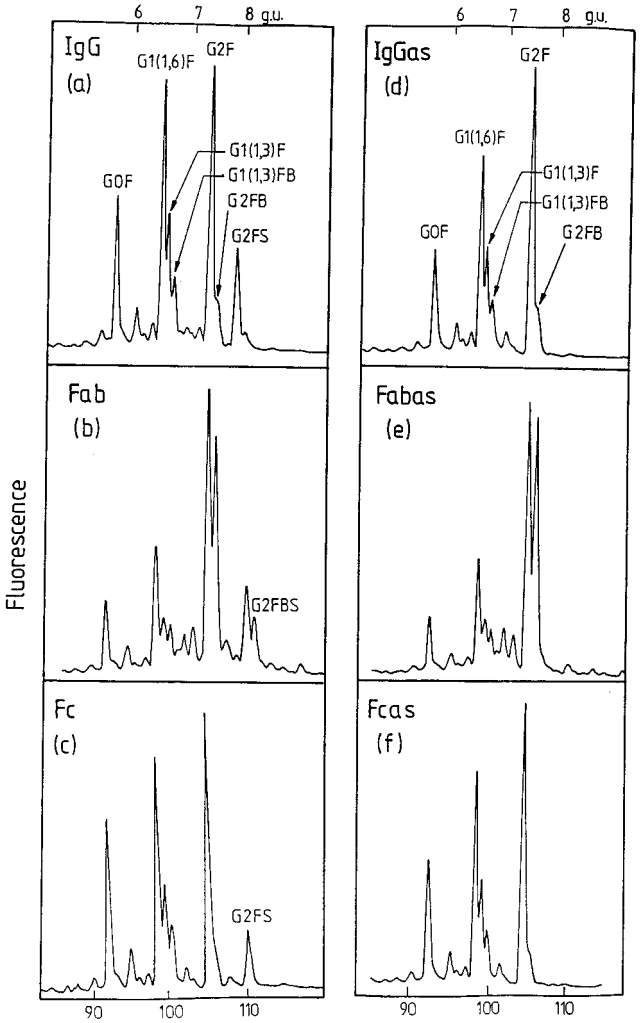


FIGURE 2: Panels a−c show the HPLC analysis of the glycan pool released from normal human serum IgG, Fab, and Fc, respectively. Panels d−f show the HPLC analyses of the corresponding desialylated glycan pools from normal human serum IgG, Fab, and Fc, respectively. The assignments for some of the major peaks are indicated (see Table 1 for the full assignments and Figure 1 for the notation).

$$\sum_i [\ln[I(t)_{\text{calculated}}] - \ln[I(t)_{\text{experimental}}]]^2$$

*Molecular Modeling.* Molecular graphics and modeling were performed on a Silicon Graphics Personal Iris workstation using the programs Insight II and Discover (Biosym Technologies Ltd.). Protein X-ray crystal structures were obtained from the Chemical Database Service at Daresbury (Fletcher et al., 1996). IgG Fc containing G2 type oligosaccharides was modeled from the crystal structure of human IgG Fc (Deisenhofer, 1981) [which contains G1(1,6)F oligosaccharides] by adding an extra $\beta$-galactose to the 4 position of the 1,3 arm GlcNAc, using the same glycosidic linkage torsion angles as for the 1,6 arm Gal$\beta$1−4GlcNAc linkage (from the crystal structure).

## RESULTS

*Separation and Identification of IgG Glycans.* The normal phase HPLC separations of the total glycan pools released from normal human serum IgG, Fab, and Fc, together with the corresponding desialylated glycan pools are shown in Figure 2 and the data summarized in Table 1. Figure 3 and Table 2 show the HPLC separation of the total glycan pools

Table 1: Relative Proportions of the Desialylated Glycan Populations from Normal Human Serum IgG, Fab, and Fc[a]

| | | relative glycan population | | | |
|---|---|---|---|---|---|
| | | experimental | | | calcd[b] |
| gu value | oligosaccharide | Fc | Fab | IgG | IgG |
| 5.42 | G0 | 0.7 | 0.2 | 1.0 | 0.6 |
| 5.61 | G0B | 1.5 | 0.7 | 2.0 | 1.4 |
| 5.82 | G0F | 15.7 | 5.2 | 13.8 | 13.9 |
| 6.12 | G0FB | 4.0 | 1.6 | 3.9 | 3.6 |
| 6.24 | G1(1,6) | 1.5 | 0.1 | 1.4 | 1.3 |
| 6.39 | G1(1,3) + G1(1,6)B | 2.2 | 1.0 | 2.6 | 2.0 |
| 6.59 | G1(1,3)B + G1(1,6)F | 20.2 | 11.2 | 18.9 | 18.7 |
| 6.73 | G1(1,3)F + G1(1,6)FB | 10.6 | 5.2 | 9.7 | 9.7 |
| 6.82 | G1(1,3)FB | 6.3 | 4.2 | 6.3 | 6.0 |
| 7.04 | G2 | 2.8 | 5.4 | 3.8 | 3.2 |
| 7.2 | G2B | 0.5 | 4.9 | 1.3 | 1.2 |
| 7.4 | G2F | 30.0 | 29.3 | 29.0 | 29.9 |
| 7.5 | G2FB | 4.0 | 31.0 | 6.3 | 8.5 |
| overall | G0(%) | 22.0 | 7.7 | 20.7 | 19.5 |
| | G1(%) | 40.8 | 21.7 | 38.9 | 37.7 |
| | G2(%) | 37.2 | 70.6 | 40.4 | 42.8 |

[a] For the notation, see Figure 1. [b] The calculated glycan populations for intact IgG based on the experimental glycan populations for Fab and Fc and assuming 2 Fc oligosaccharides and 0.4 Fab oligosaccharides per molecule.

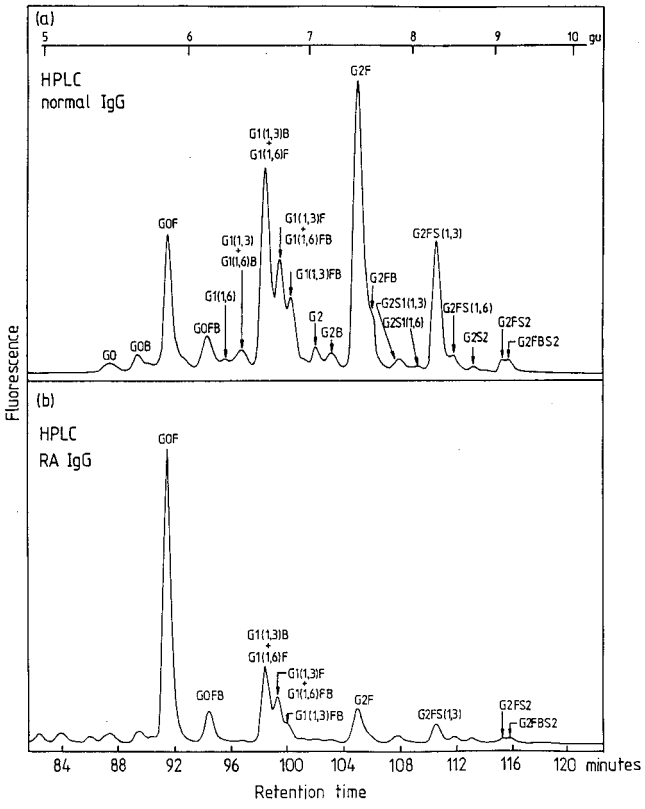


FIGURE 3: Comparison of the profiles of the glycan pools released from normal (a) and RA (b) IgG, showing the peak assignments for the major glycans (see Table 2 for the full assignments and Figure 1 for the notation).

derived from normal human serum IgG and RA IgG. The peaks containing G0 and G2 type sugars were assigned by a combination of MALDI MS analysis, HPLC using coinjections with standard sugars, and sequential exoglycosidase digestions (Guile et al., 1996). In contrast to previous oligosaccharide separation techniques, the HPLC protocol used here is able to resolve a G1 type sugar which has the galactose on the 1,3 arm from that with the galactose on the 1,6 arm [for example, G1(1,3)F can be resolved from G1(1,6)F]. There is still some residual overlap between different G1 type sugars [for example, G1(1,3)F overlaps with G1(1,6)FB], but these can be easily distinguished by mass spectrometry. The arm-specific isomers of the G1 type sugars were assigned by MALDI MS using in-source decay and high-energy collisional-induced decomposition (CID). In-source decay fragmentation spectra (Harvey et al., 1995) from both isomers were similar with Y type glycosidic cleavages (Domon & Costello, 1988), confirming the presence of one hexose (galactose) residue. This residue was located on the 1,6 arm of the first isomer to elute from the HPLC column as shown by the presence of an ion at *m/z* 712 in its spectrum. This ion has been shown in earlier work (unpublished) to originate by loss of the antenna attached to the 3 position of the branching mannose together with both core GlcNAc residues. In the spectrum of the other isomer, the ion at *m/z* 712 was missing but was replaced by an ion 162 mass units lower at *m/z* 550. This mass difference corresponds to the absence of one hexose (galactose) residue. The ratio of the ions at *m/z* 712 and 550 in the CID spectra of the two isomers (Figure 4) paralleled that seen in the ISD spectra, and further evidence for the assignment of the galactose residue to the first HPLC peak was obtained from the presence of a $^{3,5}A_4$ cross-ring cleavage ion (Domon & Costello, 1988) at *m/z* 624 (Figure 4c). Although weak, this ion is consistently seen at an equivalent relative abundance in the spectra of other N-linked carbohydrates, and its mass is diagnostic of the composition of the 1,6 arm.

Table 2: Relative Proportions of the Glycan Populations from Normal and RA Serum IgG[a]

| | | relative glycan population | |
|---|---|---|---|
| gu value | oligosaccharide | normal | RA |
| 5.42 | G0 | 1.1 | 2.3 |
| 5.61 | G0B | 1.8 | 2.1 |
| 5.82 | G0F | 11.4 | 43.9 |
| 6.12 | G0FB | 4.3 | 6.8 |
| 6.24 | G1(1,6) | 0.2 | 0.0 |
| 6.39 | G1(1,3) + G1(1,6)B | 2.8 | 0.8 |
| 6.59 | G1(1,3)B + G1(1,6)F | 16.8 | 13.8 |
| 6.73 | G1(1,3)F + G1(1,6)FB | 8.3 | 9.7 |
| 6.82 | G1(1,3)FB | 5.9 | 2.0 |
| 7.04 | G2 | 1.9 | 0.7 |
| 7.2 | G2B | 1.9 | 0.7 |
| 7.4 | G2F | 27.0 | 7.8 |
| 7.5 | G2FB | 2.0 | 0.4 |
| 7.86 | G2S1(1,3) | 1.5 | 1.6 |
| 8.06 | G2S1(1,6) | 0.3 | 0.2 |
| 8.26 | G2FS1(1,3) | 9.9 | 3.7 |
| 8.45 | G2FS1(1,6) + G2FBS1(1,3) | 1.3 | 1.2 |
| 8.7 | G2S2 | 0.6 | 0.9 |
| 9.05 | G2FS2 | 0.5 | 1.3 |
| 9.13 | G2FBS2 | 0.5 | 0.1 |
| overall | G0(%) | 18.7 | 55.2 |
| | G1(%) | 33.9 | 26.2 |
| | G2(%) | 47.4 | 18.6 |

[a] For the notation, see Figure 1.

*Site-Specific Glycosylation of Fab and Fc.* The glycosylation profile of Fab (Figure 2b) shows two dominant species, G2F and G2FB. These two together account for 60% of the desialylated glycan pool (Table 1). There are four other species with significant populations present on the Fab: G0F, G1(1,6)F, G2FS, and G2FBS. The glycosylation profile of Fc (Figure 2c) shows three major species: G0F, G1(1,6)F, and G2F. These three together account for 65% of the

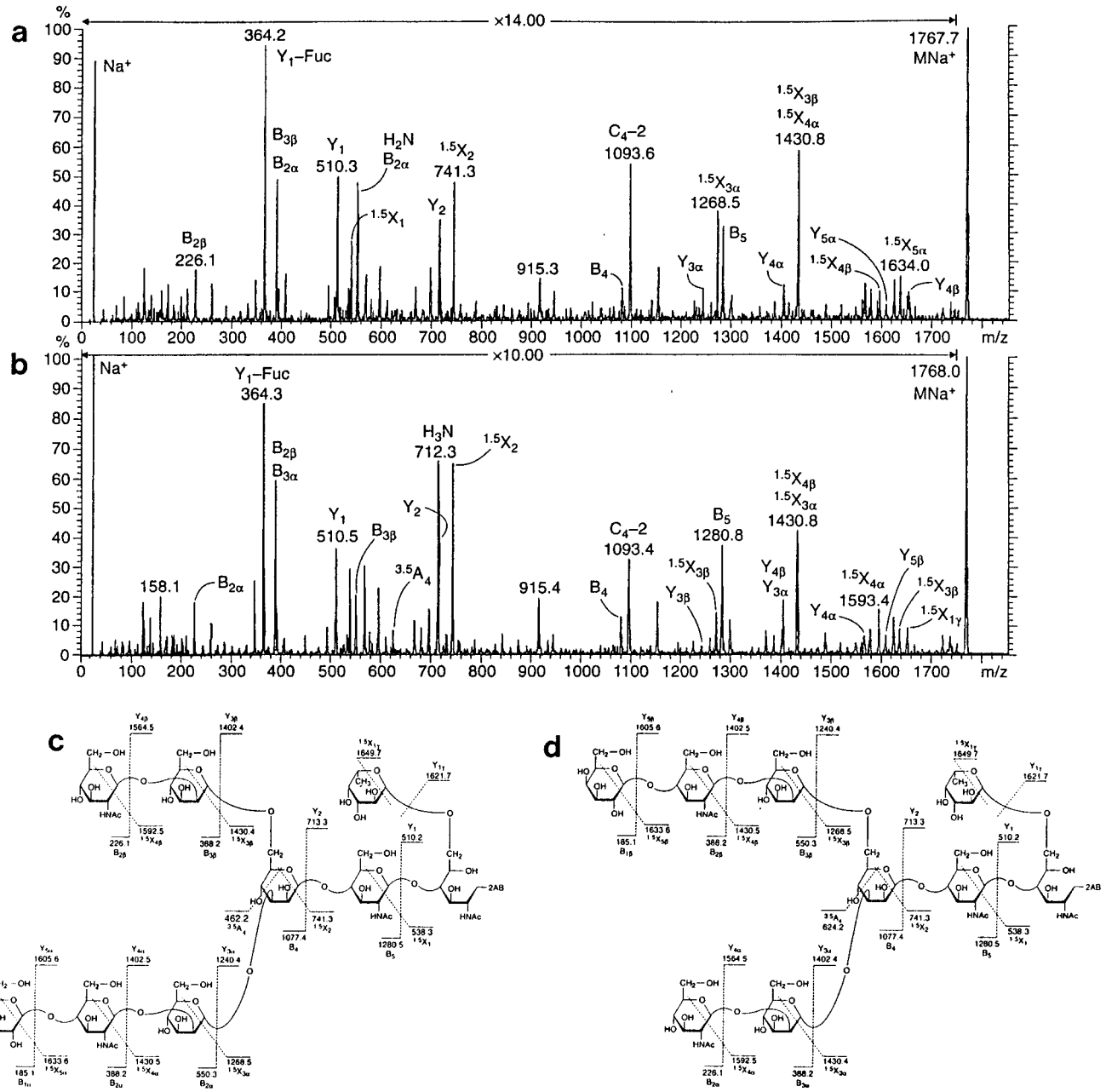


FIGURE 4: Panels a and b show the 800 eV CID MALDI mass spectra of the G1 isomers having the galactose on the 1,3 and 1,6 arm, respectively. Panels c and d show the cleavages that produce the major significant ions in the two spectra. For the ions marked $H_2N$ and $H_3N$, H = hexose and N = GlcNAc. These ions contain the 1,6 arm and branching mannose residues.

desialylated glycan pool (Table 1). There is one other species with a significant population present on the Fc, G2FS.

The observed glycosylation profile for intact IgG (panels a and d of Figure 2) can be reproduced by combining the glycosylation profiles of Fc and Fab in the ratio 2:0.4. This calculation for the desialylated glycan pools is given in Table 1. Thus, Fab-derived glycans account for only about 17% of the total glycan pool, consistent with previous reports (Youings et al., 1996).

Compared to that of Fc, the Fab glycan population contains a higher proportion of G2 type sugars (71%:37%) and fewer G1 (22%:41%) and G0 type sugars (8%:22%). The Fab glycan pool also contains a higher proportion of sugars with a bisecting GlcNAc residue, the ratio of G2F to G2FB being 1:1 for Fab compared to 5:1 for Fc (Table 1). Almost 90% of the G2FB sugars observed in IgG are derived from the Fab fragment. Consistent with this, Fab contains a population of monosialylated G2FB sugars (Figure 2b) not detected in Fc (Figure 2c).

The relative HPLC profile intensities for the G1 type oligosaccharides (6.24−6.82 gu) of Fab and Fc are very similar (Figure 2 and Table 1), showing that the relative proportions of the arm-specific G1 populations in the Fab and Fc are similar. The populations of the nonfucosylated structures are very low (typically about 1.5% for Fc; see Table 1). Thus, the peak at 6.59 gu contains mostly G1-(1,6)F. Comparison of this peak with the peak at 6.73 gu, which is the superposition of two fucosylated structures, gives an overall G1(1,3):G1(1,6) ratio of approximately 1:4. This can be compared with previously reported values of G1(1,3):G1(1,6) of 1:3 for mouse IgG (Mizuochi et al., 1987) and 1:6 for human IgG (Parekh, 1987). In these latter studies, the separate oligosaccharides could not be resolved by chromatographic techniques and relied on enzymatic or

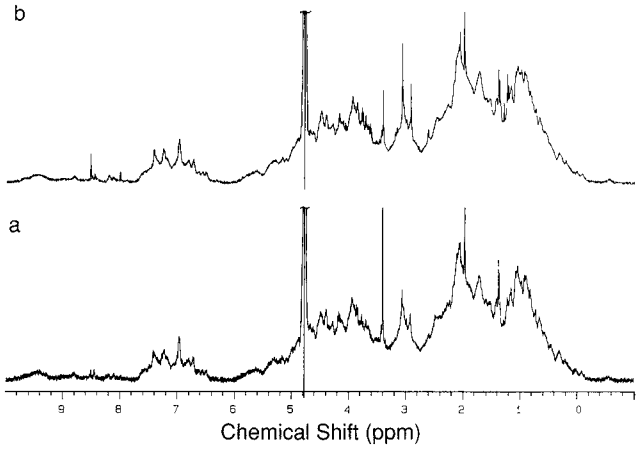


FIGURE 5: 1D $^1$H NMR spectra of IgG Fc from normal and rheumatoid samples. Both spectra were recorded in $^2H_2O$ at 500 MHz and at a probe temperature of 30 °C: (a) normal sample at pH 6.2 and (b) rheumatoid sample at pH 6.0.

chemical degradation to separate the arm-specific isomers.

There are also more sialylated glycans in Fab. This simply reflects the much larger incidence of G2 type oligosaccharides in Fab, since the proportion of G2 type oligosaccharides which are sialylated is similar in Fab and Fc (panels b and c of Figure 2). It is very interesting to note that for IgG the ratio of G2S1(1,3) to G2S1(1,6) type glycans is 5:1 (Table 2), in contrast to the ratio of G1(1,3) to G1(1,6) type glycans of 1:4. Inspection of panels b and c of Figure 2 shows that all the monosialylated glycans with 1,6 arm sialylation are found on the Fab, Fc glycans only showing 1,3 arm sialylation. Consistent with this, almost all of the disialylated glycans found in IgG are present on the Fab (panels b and c of Figure 2).

*Comparison of the Glycosylation of Normal and RA IgG.* The glycosylation profiles of IgG from a normal control and an RA patient are given in Figure 3. The increase in the total G0(%), obtained by comparing the appropriate peak areas, is from 19 to 55 (Table 2). There is a marked decrease (Figure 3 and Table 2) in the ratio of G2FS(1,3) to G2FS-(1,6) and G2FBS(1,3) from 10:1 to 4:1 between normal and RA IgG.

The HPLC pattern of the G1 type oligosaccharides isolated from the serum of 17 RA patients (for a typical example, see Figure 3b) showed no significant differences when compared with that of normal IgG (Figure 3a). This indicates that the 1,3 to 1,6 arm galactosylation ratio has not changed.

*NMR Results.* The 1D $^1$H NMR spectra of normal and rheumatoid IgG Fc (Figure 5) are very similar. Most resonances are relatively broad, but a set of weak, much sharper resonances can be seen in both spectra between 3.5 and 4.25 ppm [peptide α-CH and oligosaccharide ring (C2H−C6H) region]. These sharp peaks appear to be more intense in the rheumatoid sample. Figure 6 shows the aliphatic regions of the CPMG spectra of the rheumatoid sample at a very short total delay time (effectively the 1D spectrum) and a long total delay time. The set of sharper resonances can be seen very clearly in the latter.

Because of the very considerable resonance overlap, it is not possible to identify individual peaks to determine their $T_2$ times. The approach used is analysis of entire regions of the spectrum to obtain average $T_2$ values for particular sets of resonances and thus generate a coarse mobility map for regions of the protein structure. Plots of In($I$) versus $t$,

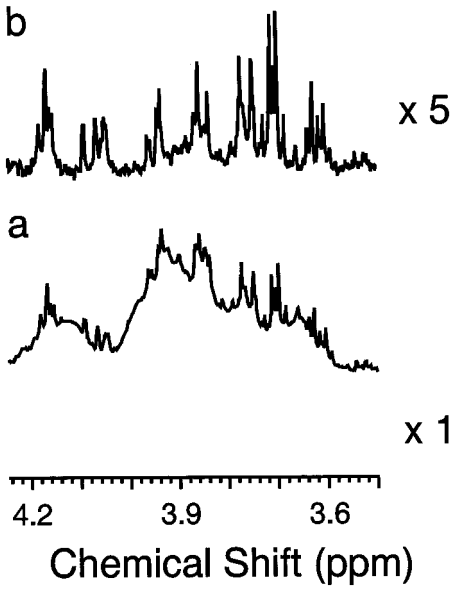


FIGURE 6: Aliphatic region of the $^1$H CPMG spectra of the IgG Fc rheumatoid sample. Spectra were recorded in $^2H_2O$ at pH 6.0 and 500 MHz and at a probe temperature of 30 °C; the total spin echo time = 0.001 s (a) and 0.128 s (b). Spectrum b is plotted at a vertical expansion of 5 times relative to spectrum a.

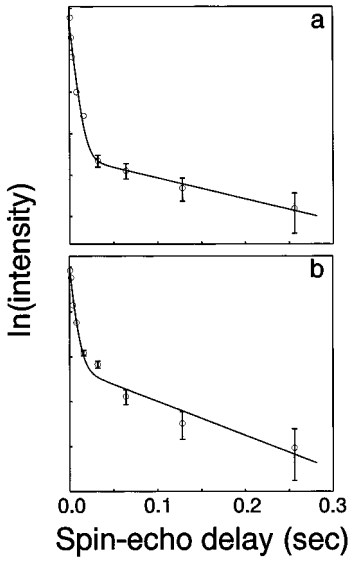


FIGURE 7: Plots of In(intensity) (arbitrary scale) versus total spin echo delay time (seconds) obtained from the CPMG spectra. The circles give the experimental data points, and the lines give the biexponential fits to the experimental data (see Table 3): (a) normal aliphatic region and (b) rheumatoid aliphatic region.

obtained from the CPMG spectra, for the aliphatic regions of both samples are shown in Figure 7 (circles) together with the fitted curve (solid line), and the fitted values of $T_2$ and $I°$ for all regions are given in Table 3. The data for the aromatic and aliphatic regions can be fitted well using a biexponential decay, although the aliphatic region of the rheumatoid sample shows some small signs of multiexponential behavior (Figure 7b). The decay curves for the methyl region are more complex and thus should be treated with some circumspection. In particular, the rheumatoid sample contained some small molecular weight impurities in this region. The only significant change between the two samples is the doubling in intensity of the second aliphatic $T_2$ component.

Table 3: Results of the CPMG Analysis for the Normal and Rheumatoid Serum IgG Fc Samples[a]

| CPMG analysis | | IgG Fc normal | IgG Fc rheumatoid |
|---|---|---|---|
| aromatic region (6.19−7.80 ppm) | | | |
| component 1 | intensity | 0.882 (164) | 0.889 (165) |
| | $T_2$ (s) | 0.008 | 0.006 |
| component 2 | intensity | 0.118 (22) | 0.111 (21) |
| | $T_2$ (s) | 0.052 | 0.090 |
| aliphatic region (3.50−4.25 ppm) | | | |
| component 1 | intensity | 2.215 (412) | 1.956 (364) |
| | $T_2$ (s) | 0.005 | 0.006 |
| component 2 | intensity | 0.095 (18) | 0.218 (41) |
| | $T_2$ (s) | 0.197 | 0.134 |
| methyl region (1.33 to −0.67 ppm) | | | |
| component 1 | intensity | 11.3 (2102) | 9.4 (1748) |
| | $T_2$ (s) | 0.001 | 0.001 |
| component 2 | intensity | 0.62 (115) | 0.81 (151) |
| | $T_2$ (s) | 0.032 | 0.019 |
| component 3 | intensity | − | 0.028 (5) |
| | $T_2$ (s) | − | 0.488 |

[a] The intensity values are normalized to give a total intensity of 1 unit for the aromatic region. The values in parentheses give the intensity in numbers of protons (based on 186 protons per molecule in the aromatic region from the amino acid sequence). The fitted values for the methyl region give considerably worse fits to the experimental data than the values for the aromatic or aliphatic regions.

Table 4: Results of the Analysis of the Pool of Released Oligosaccharides from the Normal and Rheumatoid Serum IgG Fc Samples Used for the NMR Studies[a]

| glycoform population | IgG Fc normal | IgG Fc rheumatoid |
|---|---|---|
| G0(%) | 26.0 ± 2.4 | 55.2 ± 3.0 |
| G1(%) | 46.5 ± 1.5 | 29.8 ± 1.2 |
| G2(%) | 27.5 ± 4.0 | 15.0 ± 4.2 |

[a] Data given are the average of two values.

IgG Fc lacking all galactose was prepared enzymatically, but this proved to be too insoluble for us to obtain sufficiently concentrated solutions for NMR. Attempts were also made to study isolated IgG Fab fragments. However, with an average of 0.2 glycans per Fab, this would require a 10-fold higher protein concentration than for Fc which proved to be impractical.

*Terminal Galactose Analysis of the NMR Samples.* The normal and rheumatoid IgG Fc samples were subjected to chemical release of the oligosaccharides (hydrazinolysis) followed by analysis of the pool of released oligosaccharides. The oligosaccharides were classified according to the number of outer arm galactose residues present. This shows a doubling of the G0(%) value in the RA sample relative to that of normal serum IgG, with the incidence of the other glycoforms decreasing (Table 4).

*Mathematical Modeling of the CPMG Results.* The second aliphatic $T_2$ component can be associated with oligosaccharide protons (see Discussion). Considering the three major glycan structures on Fc, if the number of slowly relaxing protons per glycoform is $x$ for G0, $y$ for G1(1,6), and $z$ for G2 type oligosaccharides, then the total number ($N$) of slowly relaxing protons per molecule in each glycoform ensemble (see Table 3) is given by

$$2[\text{fraction(G0)}x + \text{fraction(G1)}y + \text{fraction(G2)}z] = N$$

The factor of 2 allows for two oligosaccharide chains per molecule. This gives for the normal sample

$$2(0.26x + 0.465y + 0.275z) = 18$$

and for the rheumatoid sample

$$2(0.55x + 0.30y + 0.15z) = 41$$

Given the criteria that $x$, $y$, and $z$ must all be equal to or greater than zero, there are no exact solutions to this set of equations. The closest solution that meets the above criteria is $x = 36$, $y = 0$, and $z = 0$, giving values of $N$ for the two ensembles to within ±1 proton of the experimental values. Any other solution with $y$ and/or $z$ greater than zero results in a larger value for $x$. Thus, each G0 type oligosaccharide contains a minimum of 36 slowly relaxing protons (equivalent to six of the eight monosaccharide residues for G0F).

## DISCUSSION

The glycosylation profile of a glycoprotein depends on a number of factors, including (i) the absolute levels of the glycan-processing enzymes present within the cell and competition between them for substrates, (ii) the competition between glycans on different sites for the enzymes, and (iii) the glycoprotein three-dimensional structure and peptide−glycan interactions which can provide partial or complete protection of the glycan from the enzymes. The comparison between Fab and Fc glycosylation allows the role of the protein tertiary and quaternary structure in controlling glycan processing to be investigated in the presence of constant enzyme levels.

The HPLC analysis shows that there are at least 24 glycan structures found on IgG (Table 2). There are three major glycan structures present on Fc and two on Fab, in both cases accounting for over 60% of the desialylated glycan pool. For the Fc, all other species are present at less than 6% in the desialylated glycan pool (Table 1). This contrasts with the very large heterogeneity found in other glycoproteins in the immune system, for example over 130 glycan structures on the single N-glycosylation site on CD59 (Rudd et al., 1996). Unrestricted glycan processing leads to a very large number of possible glycan structures (as observed for CD59). Observation of a limited number of glycoforms implies that considerable restrictions are being placed on the glycan processing.

Fab contains relatively more galactose and bisecting GlcNAc than the Fc. This suggests that the accessibility of the glycans to the galactosyltransferase and GlcNAcV transferase enzymes is determined by the local protein structure, indicating that the nonreducing terminal arms of the Fc oligosaccharides are partially protected by the protein structure at these stages of the biosynthetic pathway.

The ratio of 1,3 arm to 1,6 arm galactosylation of 1:4 for the IgG glycans is the reverse of the observed *in vitro* specificity (6:1) of Gal$\beta$1→4 transferase for Asn-linked oligosaccharides (Narasimhan et al., 1985). The presence of bisecting GlcNAc, as is found on Fab glycans but not Fc, is known to reduce 1,3 arm relative to 1,6 arm galactosylation to 3:1 (Narasimhan et al., 1985). This would still not account for the predominance of 1,6 arm galactosylation in Fab (Figure 2b). The observation of high levels of bisecting GlcNAc, galactosylation, and disialylation indicates that both arms of the Fab glycans are easily accessible, consistent with the X-ray and ESR data showing these glycans to be mobile. Thus, the protein is not likely to play a role in determining

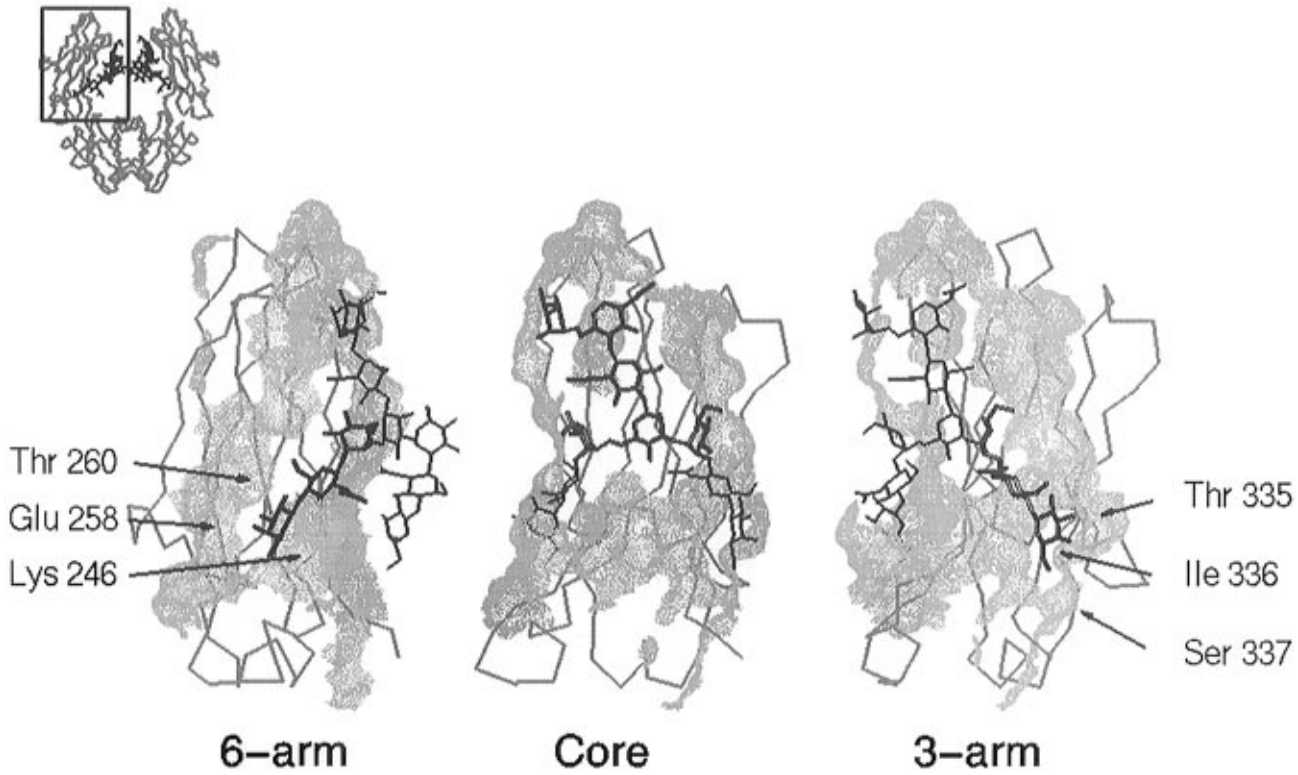


FIGURE 8: IgG Fc crystallographic oligosaccharide−protein interactions: (top left) structure of human IgG Fc (Deisenhofer, 1981), showing the peptide backbone trace (gray) and oligosaccharide (black) with one of the $C_H2$ domains boxed, and (main figure) $C_H2$ domain solvent accessible peptide surfaces for the regions covered by a G2F oligosaccharide 1,6 arm (left), core (middle), and 1,3 arm (right).

arm specificity, suggesting that the galactosyltransferase arm specificity is altered in the cell relative to the *in vitro* conditions. The absence of bisecting GlcNAc in the Fc glycans should still lead to more 1,3 arm galactosylation compared to that in Fab. This is not found to be the case. This can be explained by the Fc quaternary structure resulting in differential access to the two glycan arms. The position of the glycosylation site within the protein structure (indicated by a square in Figure 9) allows displacement of the 1,6 arm from between the $C_H2$ domains while the 1,3 arm is still inaccessible.

Decreased galactosylation is observed in the total glycan pool of RA compared to normal IgG. The decreased level of galactosylation associated with rheumatoid arthritis affects both the 1,6 and 1,3 arms equally. Thus, the differences in galactosyltransferase levels or activities which have been noted in RA (Furukawa et al., 1990) appear not to affect the galactosyltransferase arm specificity. However, not all the galactosylated glycans show the same decrease in incidence. As noted above, the ratio of G2FS(1,3) to G2FS(1,6) and G2FBS(1,3) decreases from 10:1 to 4:1 between normal and RA IgG. 1,6 arm sialylation and the presence of bisecting GlcNAc residues are associated with Fab glycans, while the majority of G2FS(1,3) glycans come from the Fc. Thus, this suggests that there is little or no decrease in the amount of Fab G2 type sugars in RA, the reduced galactosylation only affecting the Fc glycans, consistent with previous reports (Youings et al., 1996).

The 1D NMR spectrum of a protein is a good "fingerprint" of an overall protein structure. From the similarity of the 1D spectra (Figure 5), it is clear that there are no major structural changes between IgG Fc isolated from a normal and rheumatoid arthritic patient.

Measurement of proton transverse relaxation rates (Figure 6 and Table 3) allowed us to probe in more detail the dynamic behavior of regions of the protein structure. Most protons in both samples have transverse relaxation times of 0.001−0.008 s, corresponding to protons moving at the bulk tumbling rate of the protein with no extra internal motion. The second aromatic $T_2$ component contains protons with a greater degree of motion than either the peptide backbone or the bulk of the aromatic side chains, probably corresponding to aromatic side chains undergoing ring flipping (rotation by 180° about the $C\beta-C\gamma$ bond) within the protein structure. Again this is unchanged between the two samples, indicating that environments of the aromatic residues (dispersed through the cores of the $C_H2$ and $C_H3$ domains and the interface between the two $C_H3$ domains) have not changed.

The second aliphatic $T_2$ component in both samples has a much slower relaxation rate than any other peaks in either spectrum and must correspond to residues with a very high degree of dynamic freedom. From the chemical shift dispersion of these resonances and the lack of similar sharp resonances in any other region of the spectrum, these can be associated with the oligosaccharide ring protons. Their $T_2$ values of 0.1−0.2 s are also comparable with typical values (0.2−0.5 s) observed for released oligosaccharides of a similar size. The oligosaccharides present on the Fc contribute approximately 90 protons to this region of the spectrum, compared to either 18 or 41 protons in the second $T_2$ component. Thus, the majority of oligosaccharide residues in both samples must have relaxation properties similar to those of the peptide backbone, consistent with previous $^{13}C$ NMR and ESR studies and the X-ray structural data. The presence of a small, more mobile oligosaccharide population has not previously been reported.

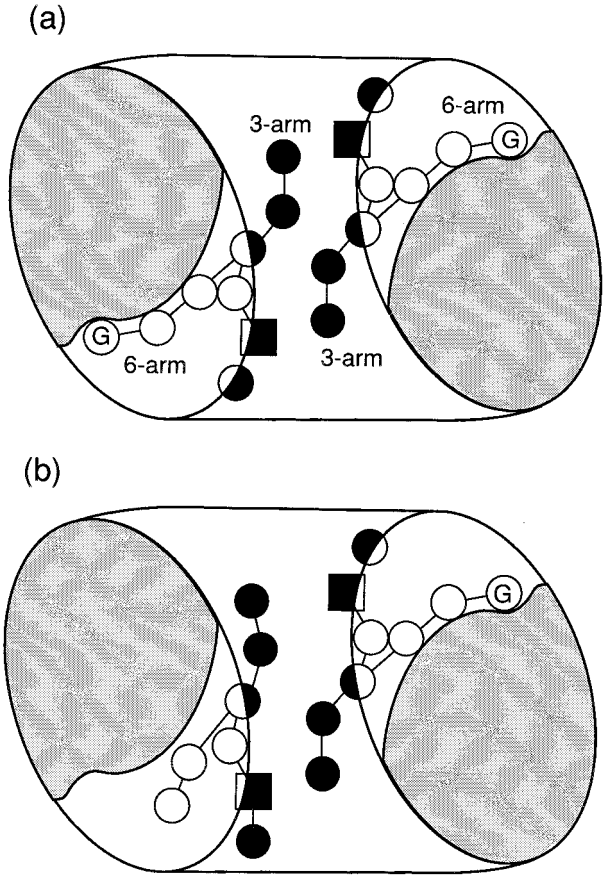


FIGURE 9: Schematic representation of the oligosaccharides of IgG Fc. The squares show the positions of the GlcNAc 1 residues (covalently linked to the protein), and the circles show the positions of the other monosaccharide residues; G indicates nonreducing terminal galactose residues on the 1,6 arm of the oligosaccharide. (a) Two fucosylated monogalacto-biantennary oligosaccharides [IgG(G1,G1) glycoform]. The 1,6 arm of each oligosaccharide is bound to the surface of the protein via the nonreducing terminal galactose residue. This results in both oligosaccharides being held rigidly in place and the 1,3 arms pointing toward each other. (b) A fucosylated agalacto-biantennary (left) and a fucosylated monogalacto-biantennary (right) oligosaccharide [IgG(G0,G1) glycoform]. The 1,6 arm of an oligosaccharide missing the nonreducing terminal galactose residue is no longer bound to the protein surface, and thus, the whole oligosaccharide can move around the covalent linkage point.

The doubling in intensity (Table 3) of the slowly relaxing oligosaccharide component between the normal and rheumatoid samples mirrors a doubling of the G0(%) value (Table 4) between the two samples (in fact, the incidence of every other glycoform decreases). This suggests that the slowly relaxing oligosaccharide component consists of G0 type oligosaccharides, G1 and G2 type oligosaccharides having relaxation properties similar to those of the peptide backbone. Mathematical modeling of the CPMG data (above) is fully consistent with this model and also indicates that both arms of the G0 type glycans have increased mobility.

The crystal structure of human IgG Fc [containing G1-(1,6)F oligosaccharides] clearly shows extensive interactions between the 1,6 arm galactose [present in G1(1,6) and G2 but not in G0 type glycans] and the protein surface (Figure 8, bottom left). The crystal structure also shows interactions between the oligosaccharide core and the protein surface (Figure 8, bottom middle).

Modeling of the position of the 1,3 arm galactose (Figure 8, bottom right) shows that G2 type glycans can be accommodated by the crystal structure. There is a hydrophobic area of protein surface with which the hydrophobic face of the galactose residue could interact. However, this interaction would not be nearly as extensive as for the 1,6 arm (Figure 8, bottom left and bottom right). This is consistent with the observation that sialylation of Fc glycans can occur on the 1,3 arm but not on the 1,6 arm. In this case, it is the glycan−protein interactions, rather than just the protein quaternary structure, which are restricting glycosylation.

The NMR data indicate that, once the interactions involving the 1,6 arm galactose residue are lost, most residues of the glycan become mobile. Thus, the interactions between the oligosaccharide core and the protein are not sufficient to hold the oligosaccharide to the protein surface (shown in Figures 9 and 10). In fact, if the core interactions were sufficient to hold the glycan in its crystallographic position, then it would be completely protected from glycan processing.

It is interesting to note that the average $T_2$ of the mobile oligosaccharide component from the rheumatoid sample is slightly shorter than that from the normal sample. This may be due to a significant proportion of rheumatoid Fc molecules having two mobile saccharide chains which could interfere with each other. This may also account for the slightly worse fit of the CPMG data for the aliphatic region of this sample to a biexponential decay (see above).

The relaxation measurements do not give any information about the amplitude of these motions (except that they must be large enough to cause significant averaging of the proton's magnetic environment). The observation of galactosylation of Fc G0 type glycans *in vivo* (above) and the recognition of these glycans by MBP *in vitro* (Malhotra et al., 1995) indicate that the glycans can be displaced significantly from their crystallographic position toward the exterior of the protein. However, the observation of reduced galactosylation relative to Fab indicates that the glycans still spend part of the time in the space between the $C_H2$ domains.

## CONCLUSIONS

The assembly of the IgG quaternary structure occurs in the endoplasmic reticulum (Bole et al., 1986) before extensive glycan processing takes place. The glycosylation pattern of IgG is strongly influenced by the protein three-dimensional structure, giving rise to a very limited range of glycans. At the early stages of biosynthesis, the mobility of the Fc glycans makes them accessible for processing, although their position in the protein quaternary structure (between the $C_H2$ domains) still leads to partial protection. This results in glycan processing occurring to give complex type oligosaccharides but with little bisecting GlcNAc, reduced galactosylation, and preferential galactosylation of the 1,6 arm compared to the 1,3 arm. Galactosylation of the 1,6 arm leads to strong interactions between the $C_H2$ domain and the 1,6 arm galactose residue, resulting in further sialylation only occurring on the 1,3 arm. In contrast, the more accessible Fab glycans have 5-fold higher levels of bisecting GlcNAc and higher levels of galactosylation and sialylation on both the 1,3 and 1,6 arms. The higher levels of bisecting GlcNAc also favor preferential 1,6 arm galactosylation.

The final glycosylation profile of a glycoprotein is a function of both the protein structure and the levels (or

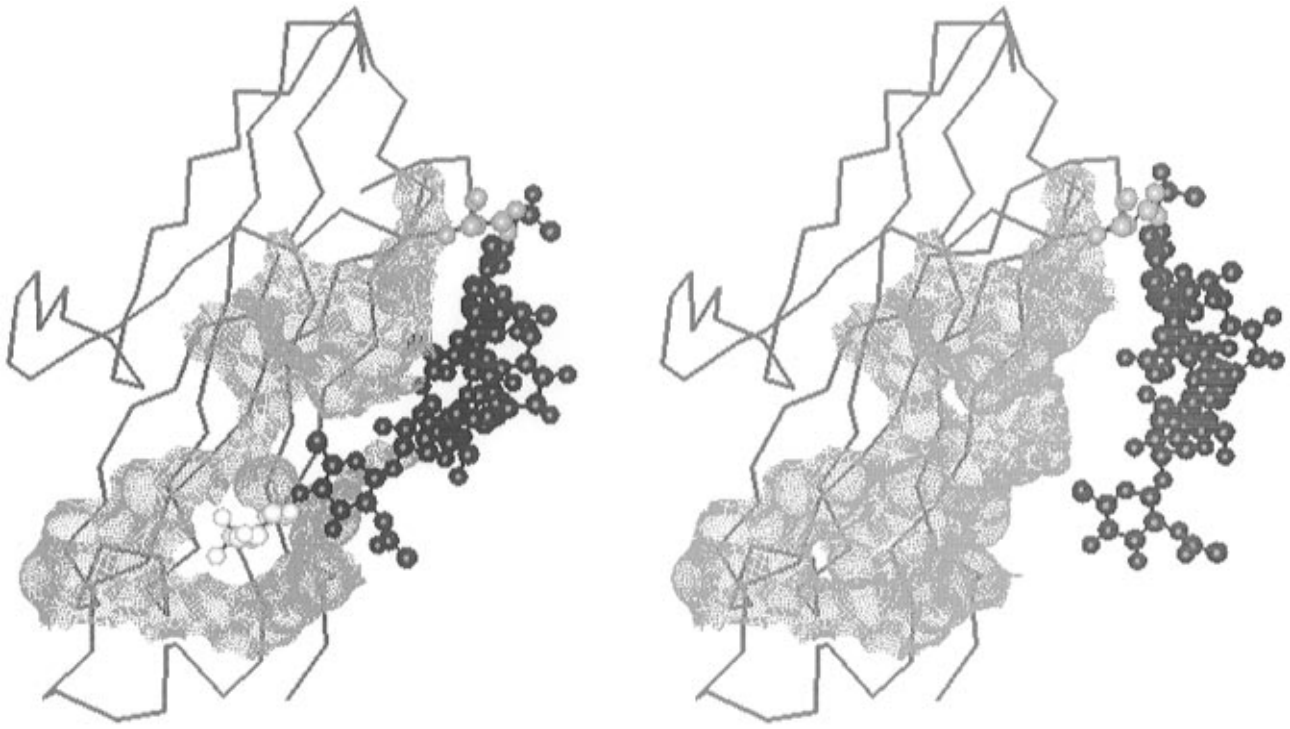

FIGURE 10: Structure of the IgG Fc $C_H2$ domain showing part of the solvent accessible peptide surface, the trace of the peptide backbone, Asn 297 (light gray), oligosaccharide (black), and the 1,6 arm terminal galactose (white): (left) a crystal structure (Deisenhofer, 1981) with a G1(1,6)F oligosaccharide showing the oligosaccharide 1,6 arm bound to the surface of the peptide and (right) a structure with a G0F oligosaccharide after allowing the oligosaccharide to move within the pocket between the two $C_H2$ domains. The newly exposed surface is formed by residues Phe 241, Phe 243, Lys 246, Glu 258, Thr 260, Val 262, and Val 264.

activities) of the glycan-processing enzymes present within the cell. The relative importance of these two factors will vary from protein to protein and from site to site for a given protein. For the partially protected (and hence less reactive) Fc glycans, the levels of galactosyltransferase activity are limiting, leading to reduced galactosylation overall and further reductions in galactosylation on reducing enzyme activities (as in RA). For the more accessible (more reactive) Fab glycans, the enzyme levels are no longer limiting and so higher levels of galactosylation are seen, with no reduction in RA.

As well as playing a role in determining glycan processing, the differential mobility of the G0, G1(1,6), and G2 type oligosaccharides in IgG Fc has important implications for both the possible molecular mechanisms associated with rheumatoid arthritis (and other diseases that are accompanied by changes in Fc glycosylation) and the normal structural role of the oligosaccharides in IgG Fc.

(i) The oligosaccharides are not responsible for keeping the two $C_H2$ domains apart. The only interactions keeping the oligosaccharides in place involve the 1,6 arm galactose residue. As the glycan becomes much more mobile on loss of this residue, there must still be space within the protein structure for it to be mobile in.

(ii) Loss of the 1,6 arm galactose residue results in changes in exposure of regions of the $C_H2$ surface, previously covered by both the galactose residue and the oligosaccharide 1,6 arm, and also in increased accessibility to the oligosaccharide previously held in place between the $C_H2$ domains (Figure 10). This is consistent with the recognition of IgG G0 glycans by MBP (Malhotra et al., 1995).

(iii) The increased mobility of the G0 type oligosaccharides suggests that they could accommodate greater induced changes in Fc quaternary structure (domain displacement) before steric interactions between the oligosaccharide chains would occur. This in turn would affect the hinge conformation and help to explain the effects of altered glycosylation on biological functions related to the hinge, such as monocyte binding or papain cleavage.

## ACKNOWLEDGMENT

We thank Dr. A. Youings for help with the oligosaccharide analysis and Dr. C. J. Edge and Dr. R. J. Woods for useful discussions. We also thank Micromass Ltd. for the use of the Autospec OA-TOF mass spectrometer. The RA IgG samples for HPLC analysis were prepared by Professor R. Jefferis as part of a study undertaken within The European Community Concerted Action for Arthritis and Carbohydrate Research. We acknowledge the use of the EPSRC's Chemical Database Service at Daresbury.

## REFERENCES

Ashford, A., Dwek, R. A., Welpy, J. K., Amatayakul, S., Homans, S. W., Lis, H., Taylor, G. N., Sharon, N., & Rademacher, T. R. (1987) *Eur. J. Biochem. 166*, 311−320.

Bateman, R. H., Green, M. R., Scott, G., & Clayton, E. (1995) *Rapid Commun. Mass Spectrom. 9*, 1227.

Bole, D. G., Hendershot, L. M., & Kearney, J. F. (1986) *J. Cell Biol. 102*, 1558−1566.

Bordoli, R. S., Vickers, R. G., Bateman, R. H., Howes, K., & Harvey, D. J. (1994) *Rapid Commun. Mass Spectrom. 8*, 585−589.

Deisenhofer, J. (1981) *Biochemistry 20*, 2361−2370.

Domon, B., & Costello, C. E. (1988) *Glycoconjugate J. 5*, 397−409.

Dwek, R. A., Lellouch, A. C., & Wormald, M. R. (1995) *J. Anat. 187*, 279−292.

Fletcher, D. A., McMeeking, R. F., & Parkin, D. (1996) *J. Chem. Inf. Comput. Sci. 36*, 746−749.

Furukawa, K., Matsuta, K., Takeuchi, F., Kosuge, E., Miyamoto, T., & Kobata, A. (1990) *Int. Immunol. 2*, 105−112.
Guile, G. R., Rudd, P. M., Wing, D. R., Prime, S. B., & Dwek, R. A. (1996) *Anal. Biochem. 240*, 210−226.
Harvey, D. J., Rudd, P. M., Bateman, R. H., Bordoli, R. S., Howes, K., Hoyes, J. B., & Vickers, R. G. (1994) *Org. Mass Spectrom. 29*, 753−766.
Harvey, D. J., Naven, T. J. P., Küster, B., Bateman, R. H., Green, M. R., & Critchley, G. (1995) *Rapid Commun. Mass Spectrom. 9*, 1556−1561.
Johnson, P. M., Watkins, J., Scopes, P. M., & Tracey, B. M. (1974) *Ann. Rheum. Dis. 33*, 366−370.
Kiyohara, T., Terao, T., Shioiri-Nakano, K., & Osawa, T. (1976) *J. Biochem. 80*, 9−17.
Lapuk, V. A., Timofeev, V. P., Tchukchrova, A. I., Khatiashvili, N. M., & Kiseleva, T. M. (1984) *J. Biomol. Struct. Dyn. 2*, 63−76.
Malhotra, R., Wormald, M. R., Rudd, P. M., Fischer, P. B., Dwek, R. A., & Sim, R. B. (1995) *Nat. Med. (N.Y.) 1*, 237−241.
Meiboom, S., & Gill, D. (1958) *Rev. Sci. Instrum. 29*, 688−691.
Mizuochi, T., Hamako, J., & Titani, K. (1987) *Arch. Biochem. Biophys. 257*, 387−394.
Narasimhan, S., Freed, J. C., & Schachter, H. (1985) *Biochemistry 24*, 1694−1700.
Newkirk, M. M., & Rauch, J. (1993) *J. Rheum. 20*, 776−780.
Nezlin, R. (1990) *Adv. Immunol. 48*, 1−40.
Parekh, R. B. (1987) D. Philos., Oxford University, Oxford.
Parekh, R. B., Dwek, R. A., Sutton, B. J., Fernandes, D. L., Leung, A., Stanworth, D., Rademacher, T. W., Mizuochi, T., Taniguchi, K., Matsuta, K., Takeuchi, Y., Nagano, T., Miyamoto, T., & Kobata, A. (1985) *Nature 316*, 452−457.
Parekh, R. B., Tse, A. G. D., Dwek, R. A., Williams, A. F., & Rademacher, T. W. (1987) *EMBO J. 6*, 1233−1244.
Parekh, R. B., Isenberg, D. A., Roitt, I. M., Dwek, R. A., & Rademacher, T. R. (1988) *J. Exp. Med. 167*, 1713−1736.
Porter, R. R. (1959) *Biochem. J. 73*, 119−126.
Rook, G. A. W., Steele, J., Brealey, R., Whyte, A., Isenberg, D., Sumar, N., Nelson, J. L., Bodman, K. B., Young, A., Roitt, I. M., Williams, P., Scragg, I., Edge, C. J., Arkwright, P. D., Ashford, D., Wormald, M., Rudd, P., Redman, C. W. G., Dwek, R. A., & Rademacher, T. W. (1991) *J. Autoimmun. 4*, 779−794.
Rosen, P., Pecht, I., & Cohen, J. S. (1979) *Mol. Immunol. 16*, 435−436.
Rudd, P. M., Morgan, B. P., Wormald, M. R., Harvey, D. J., van der Berg, C., Davis, S. J., Ferguson, M. A. J., & Dwek, R. A. (1996) *J. Biol. Chem.* (in press).
Stanfield, R. L., Fieser, T. M., Lerner, R. A., & Wilson, I. A. (1990) *Science 248*, 712−719.
Sutton, B. J., & Phillips, D. C. (1983) *Biochem. Soc. Trans. 11*, 130−132.
Sykulev, Y. K., & Nezlin, R. S. (1990) *Glycoconjugate J. 7*, 163−182.
Tsuchiya, N., Endo, T., Matsuta, K., Yoshinoya, S., Aikawa, T., Kosuge, E., Takeuchi, F., Miyamoto, Z. T., & Kobata, A. (1989) *J. Rheum. 16*, 285−290.
Uesson, M., & Hansson, U.-B. (1982) *Scand. J. Immunol. 16*, 249−256.
Watkins, J., Unger, A., & Mahon, N. (1970) *Clin. Sci. 38*, 15p−16p.
Youings, A., Chang, S.-C., Dwek, R. A., & Scragg, I. G. (1996) *J. Biol. Chem. 314*, 621−630.
Young, A., Sumar, N., Bodman, K., Goyal, S., Sinclair, H., Roitt, I., & Isenberg, D. (1991) *Arthritis Rheum. 34*, 1425−1429.

BI9621472